

Dynamical scaling analysis of the optical Hall conductivity in the quantum Hall regime

Takahiro Morimoto,¹ Yshai Avishai,^{2,3} and Hideo Aoki¹

¹*Department of Physics, University of Tokyo, Hongo, Tokyo 113-0033, Japan*

²*Department of Physics, Ben Gurion University, Beer Sheva 84105, Israel*

³*Department of Mathematics, University of Tokyo, Komaba, Tokyo 153-8914, Japan*

(Dated: April 28, 2010)

Dynamical scaling analysis is theoretically performed for the ac (optical) Hall conductivity $\sigma_{xy}(\varepsilon_F, \omega)$ as a function of Fermi energy ε_F and frequency ω for the two-dimensional electron gas and for graphene. In both systems, results based on exact diagonalization show that $\sigma_{xy}(\varepsilon_F, \omega)$ displays a well-defined dynamical scaling, for which the dynamical critical exponent as well as the localization exponent are fitted and plugged in. A crossover from the dc-like behavior to the ac regime is identified. The dynamical scaling analysis has enabled us to quantify the plateau in the ac Hall conductivity previously obtained, and to predict that the plateaux structure in ac is robust enough to be observed in the THz regime.

Introduction —

Dynamics of electrons in the integer quantum Hall effect (QHE) is an interesting, hitherto not fully explored problem. Theoretically, the question is how the static Hall conductivity, which may be regarded as a topological quantity^{1,2}, evolves into the optical Hall conductivity, especially in the THz regime where the relevant energy scale is the cyclotron energy.^{3–5} Two of the present authors and Hatsugai have recently shown that the plateau structure in $\sigma_{xy}(\omega)$ is retained in the ac (\sim THz) regime in both the ordinary two-dimensional electron gas (2DEG) and in graphene (described as the massless Dirac model), although the plateau height deviates from the quantized values in ac.⁴ The numerical result indicates that the plateau structure remains remarkably robust against disorder, which can be attributed to an effect of localization which dominates the physics of electrons around the centers of Landau levels in disordered QHE systems. However, what is physically significant is not a result for a specific sample size, but the scaling behavior, especially when the localization is relevant in disordered systems. For ac responses, we have to look into the dynamical scaling. Scaling analysis of localization-delocalization transition in the 2DEG QHE has been done for both the static *longitudinal* conductivity $\sigma_{xx}(\varepsilon_F)$, where ε_F is the Fermi energy,⁶ and for dynamical scaling properties of the longitudinal conductivity $\sigma_{xx}(\varepsilon_F, \omega)$,⁷ but the dynamical scaling for the Hall conductivity $\sigma_{xy}(\varepsilon_F, \omega)$ has not been properly addressed for both ordinary and graphene QHE.

With this motivation, here we elucidate the dynamical scaling behavior of the ac Hall conductivity around the plateau to plateau transition to gain a deeper understanding of the optical Hall effect and its robust step structures in the ac region. Namely, when we perform a scaling analysis for the plateau to plateau transition width W , the quantity depends on ω . Physically, a new length scale, $L_\omega \sim \omega^{-\frac{1}{z}}$, emerges at finite frequencies, where z is the dynamical critical exponent. We have performed the dynamical scaling analysis for both 2DEG and graphene QHE. The quantum Hall effect in graphene is unique in that a zero-energy Landau level (LL) exists,

which has no counterpart in the QHE in 2DEG⁸. Thus the dynamic scaling is of special interest for the $n = 0$ LL in graphene.

Experimentally, scaling properties of $\sigma_{xx}(\varepsilon_F, \omega)$ was investigated from $\omega = 0$ ⁹ up to the GHz regime¹⁰. Recent advances in optical measurements (e.g., Faraday rotation in magnetic fields) in the THz region have made the study of dynamical response functions feasible^{11,12}. For graphene, optical properties begin to be studied, among which are experimental transmission spectra¹³, or theoretical examination of the cyclotron emission¹⁴. Thus, the physics of dynamical scaling in graphene QHE should be interesting in the THz regime.

Here we shall show that: (i) The ac Hall conductivity obeys a well-defined dynamical scaling. (ii) There is a crossover in the scaling behavior from a dc-like regime to an ac regime, in the latter of which L_ω dominates the scaling. In the former L/ξ dominates the scaling (where ξ is the localization length), while in the latter L_ω/ξ does. (iii) The dynamical critical exponent is found to be $z \simeq 2$ in both the 2DEG and graphene QHE systems as far as the potential disorder is concerned. (iv) The analysis enables us to estimate the plateau to plateau transition width W in the ac regime with $L_\omega < L$ to assert that the Hall conductivity maintains the plateau structure at frequencies as high as $\omega \sim 0.1\omega_c$, which, for a magnetic field of a few Tesla, covers the THz region. This is an experimentally testable statement.

Formalism —

For the ordinary QHE system as typically realized in GaAs/AlGaAs, the kinetic part of the Hamiltonian is $H_0 = \frac{1}{2m^*}(\mathbf{p} + e\mathbf{A})^2$, where m^* is the effective mass of the electron, $\mathbf{p} = (p_x, p_y)$ the momentum, and \mathbf{A} the vector potential. Disorder is introduced by a random potential $V(\mathbf{r})$ composed of Gaussian scattering centers of range d and density n_{imp} placed on randomly chosen points \mathbf{R}_j :

$$V(\mathbf{r}) = \sum_j u_j \exp(-|\mathbf{r} - \mathbf{R}_j|^2/2d^2)/(2\pi d^2). \quad (1)$$

For u_j we assumed a bimodal distribution $u_j = \pm u$ with random signs so that the broadened Landau level

is symmetric. A measure of disorder, i.e., the Landau level broadening¹⁵, is $\Gamma = 2u[n_{\text{imp}}/2\pi(\ell^2 + d^2)]^{1/2}$. Here we take $d = 0.7\ell$, where $\ell = \sqrt{\hbar/eB}$ is the magnetic length, but the result does not change significantly for other choices of d . Diagonalization of the Hamiltonian is done for the subspace spanned by the five lowest LL's for $L \times L$ systems with L/ℓ varied over 25, 30, 35, 40. With wave functions and energy eigenvalues ϵ_a at hand, the optical Hall conductivity is evaluated from the Kubo formula,

$$\sigma_{xy}(\epsilon_F, \omega) = \frac{i\hbar e^2}{L^2} \sum_{\epsilon_a < \epsilon_F} \sum_{\epsilon_b \geq \epsilon_F} \frac{1}{\epsilon_b - \epsilon_a} \times \left(\frac{j_x^{ab} j_y^{ba}}{\epsilon_b - \epsilon_a - \hbar\omega} - \frac{j_y^{ab} j_x^{ba}}{\epsilon_b - \epsilon_a + \hbar\omega} \right), \quad (2)$$

where j_x^{ab} is the current matrix element⁴.

The conductance is then averaged over a few thousands samples with different disorder potential realizations. The averaged conductivity is hereafter denoted by the same symbol $\sigma_{xy}(\epsilon_F, \omega)$. For the scaling analysis the calculation done for varied sample size L , energy ϵ_F and frequency ω .

For graphene QHE, we employ the two-dimensional effective Dirac model,

$$H = v_F \boldsymbol{\sigma} \cdot \boldsymbol{\pi} + V(\mathbf{r}), \quad (3)$$

where $\boldsymbol{\sigma} = (\sigma_x, \sigma_y)$ is the Pauli matrices, $\boldsymbol{\pi} = \mathbf{p} + e\mathbf{A}$, and $V(\mathbf{r})$ the random potential¹⁶. The selection rule for the current matrix elements in the Dirac model ($|n\rangle \leftrightarrow |n| \pm 1$ with n the Landau index) is distinct from that ($n \leftrightarrow n \pm 1$) for 2DEG.

Raw results for the Optical Hall Conductivity —

The optical Hall conductivity $\sigma_{xy}(\epsilon_F, \omega)$ as a function of the Fermi energy ϵ_F and frequency ω is displayed for the 2DEG (Fig.1(a)) and graphene (Fig.1(b)) QHE systems. The density of states (DOS) for Landau levels (insets of Fig.1(a,b)) confirms that the Landau level broadening is $\simeq \Gamma$. For each value of ϵ_F , the frequency-dependence of the Hall conductivity can be recognized as the cyclotron resonance. The 2DEG has one resonance at cyclotron frequency ω_c (Fig.1(a)), while the graphene QHE system exhibits a series of resonances, which correspond to the Dirac QHE selection rule $|n\rangle \leftrightarrow |n| \pm 1$ (Fig.1(b)) for the non-uniform set of Landau levels ($\propto \sqrt{n}$). Away from a resonance, a *step-like structure* is seen in $\sigma_{xy}(\epsilon_F, \omega)$ as a function of ϵ_F even for finite values of ω , although the step heights are no longer quantized. We can attribute this behavior of $\sigma_{xy}(\epsilon_F, \omega)$ to the localization property of electrons in QHE systems: As long as $\omega \ll \omega_c, \Gamma$, the nature of the mobility gap is maintained and σ_{xy} remains flat. If we more closely inspect the width W of the plateau to plateau transition, W for a finite ω in Fig.1(d) is seen to be greater than in the static case in Fig.1(c), although still narrower than Γ .

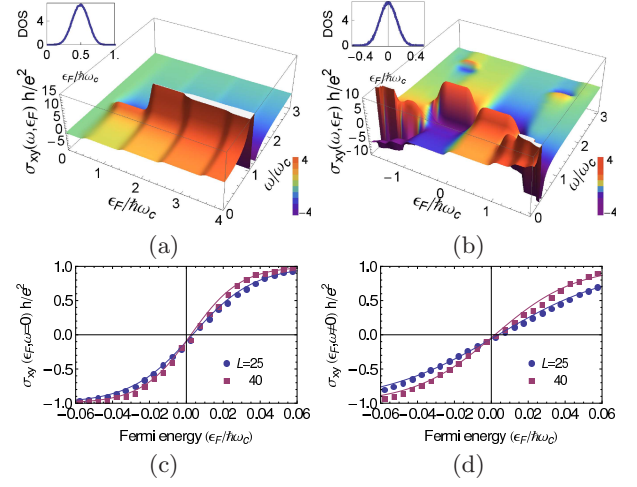


FIG. 1: $\sigma_{xy}(\epsilon_F, \omega)$ plotted against Fermi energy ϵ_F and frequency ω for (a) 2DEG, and (b) graphene quantum Hall systems for a potential disorder with $\Gamma = 0.4\hbar\omega_c$. Insets are density of states for the lowest ($n = 1$) LL (a) and $n = 0$ LL (b). (c) The static Hall conductivity $\sigma_{xy}(\epsilon_F)$ plotted against ϵ_F for the graphene QHE system of sizes $L = 25, 40$. (d) Optical Hall conductivity $\sigma_{xy}(\epsilon_F, \omega)$ plotted against ϵ_F for the graphene QHE system of sizes $L = 25, 40$ for a fixed $\omega = 6\omega_c/L^2$. The solid lines in (c) and (d) represent fitting with eqn.(5).

We now move on to the sample size dependence of the widths $W(\epsilon, \omega, L)$ for the static and dynamic Hall conductivities. For the static Hall conductivity $\sigma_{xy}(\epsilon, 0, L)$, we confirm the standard picture, where the plateau to plateau transition width becomes narrower with the sample size L as seen in Fig.1. In the thermodynamic limit, almost all the wave functions are localized, where the localization length diverges like $\xi \sim 1/|\epsilon_F - \epsilon_c|^\nu$ toward the center of the LL at $\epsilon = \epsilon_c$.¹⁷ For finite systems the states whose localization length ξ is larger than the system size L are effectively extended, and contribute to the longitudinal conductivity and the plateau to plateau transition. This suggests the behavior $W \sim L^{-1/\nu}$.

Scaling Analysis — We are now in position to look at the dynamical scaling analysis of the optical Hall conductivity $\sigma_{xy}(\epsilon_F, \omega, L)$ and the width $W(\omega, L)$ of the plateau to plateau transition. We expect that the W increasing with ω and decreasing with L may be captured with some scaling function. For that we have to quantify the width W , or the steepness ($\propto 1/W$) of the transition by fitting $\sigma_{xy}(\epsilon_F, \omega, L)$ around the transition region for a given LL to some function of ϵ_F for each value of ω . To describe the transition $\sigma_{xy}/(-e^2/h) = 0 \rightarrow 1$ in the 2DEG QHE we take

$$\sigma_{xy}(\epsilon_F, \omega, L)_{\text{2DEG}} = \frac{1}{2} + \frac{1}{2} \tanh \left[\frac{\epsilon_F - \frac{1}{2}\hbar\omega_c}{W(\omega, L)} \right], \quad (4)$$

while for the transition $\sigma_{xy}/(-e^2/h) = -1 \rightarrow 1$ in

graphene QHE we take

$$\sigma_{xy}(\varepsilon_F, \omega, L)_{\text{graphene}} = \tanh\left(\frac{\varepsilon_F}{W(\omega, L)}\right). \quad (5)$$

The quality of fitting of the plateau to plateau transition by the tanh function is quite satisfactory²¹ as can be seen in Fig.1(c,d).

Dynamical scaling analysis for $\sigma_{xy}(\varepsilon_F, \omega, L)$ is carried out in a similar manner as that for the longitudinal conductivity¹⁸. In this ansatz the optical Hall conductivity is regarded to depend on Fermi energy and frequency only through the ratios L/ξ and $L\omega/\xi$. Here we have the localization length, $\xi \sim 1/|\varepsilon_F - \varepsilon_c|^\nu$ where ε_c is the critical energy which coincides with the center of the LL, and $L\omega \sim 1/\omega^{1/z}$. Then the dynamical scaling ansatz for the optical Hall conductivity reads

$$\sigma_{xy}(\varepsilon_F, \omega, L) = \frac{e^2}{h} F((\varepsilon_F - \varepsilon_c)L^{1/\nu}, \omega L^z), \quad (6)$$

where F is a universal scaling function. This implies that the width of the plateau to plateau transition scales as

$$W(\omega, L) = L^{-1/\nu} f(\omega L^z), \quad (7)$$

where f is a universal function deduced from F . The first factor on the right-hand side makes the plateau to plateau transition width narrower for larger systems and dictates the dc scaling, while the second factor f describes the dynamical scaling.

In Fig.2 we show the scaling of inverse transition width, $1/W(\omega, L)$, for the 2DEG QHE system. By examining first the inverse width $1/W(\omega = 0)$ for the static case against system size L in Fig.2(b), we obtain the localization critical exponent ν from $\log 1/W(\omega = 0) = 1/\nu \log L + f(0)$, with the result $\nu = 2.1 \pm 0.2$. This agrees with the accepted value of the static critical exponent in the integer QHE, albeit slightly smaller.

On the other hand, the frequency dependence of the inverse width for a fixed system size L in (Fig.2(a)) clearly exhibits that there are two regions: In the first region $1/W$ stays nearly constant up to some critical frequency that depends on the system size L , while in the other the quantity begins to decrease monotonically with ω . In the latter region, $1/W$ assumes similar values for all the sample sizes studied here as shown in (Fig.2(a)). We can indeed notice that, in the first region we have $L < L_\omega$, while in the second $L > L_\omega$. If we inspect eqn.7, and assume a power-law form for the scaling function f , we can see that the inverse width in the second region should take a (L -independent) form, $1/W(\omega) \propto \omega^{-1/z\nu}$. Calculation of the dynamical exponent z should be done for the critical region (i.e. for the transition width not too large), so that we do this around the crossing region where $1/W$ begins to decrease. This happens, typically, for $\omega < 0.002\omega_c$. With a least square fitting of $\log 1/W(\omega) = \text{const} - \frac{1}{z\nu} \log \omega$, the dynamical critical exponent for the 2DEG QHE system is obtained as $z = 1.8 \pm 0.2$.

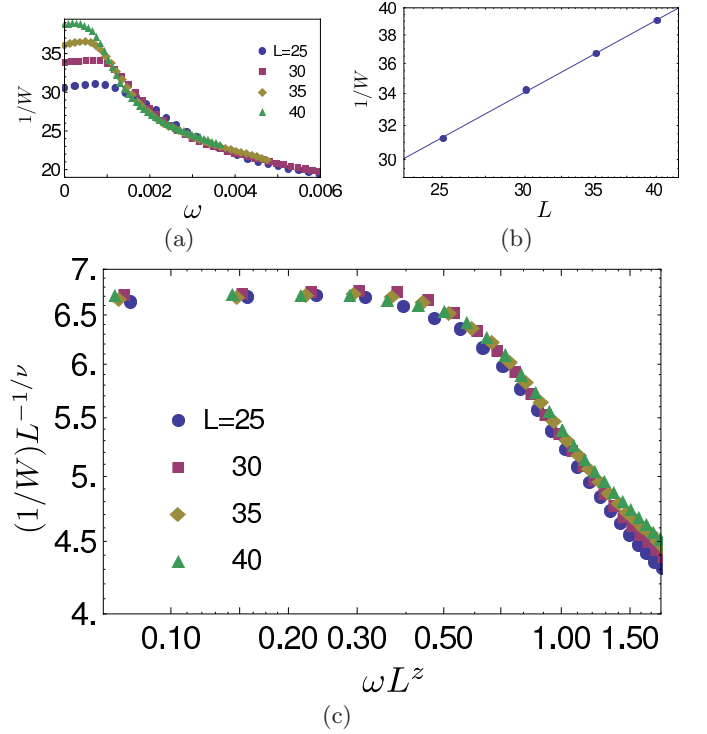


FIG. 2: Dynamical scaling analysis for the 2DEG QHE system with $\Gamma = 0.4\hbar\omega_c$ and $L = 25 - 40$: (a) The inverse width $1/W$ plotted against the frequency ω , (b) the inverse width $1/W$ plotted against the sample size L , from which the localization exponent $\nu = 2.1 \pm 0.2$ is obtained, and (c) rescaled inverse width $\frac{1}{W}L^{-1/\nu}$ plotted against the rescaled frequency ωL^z with a fitted dynamical critical exponent $z = 1.8 \pm 0.2$. W, ω, L are measured, respectively, in units of $\hbar\omega_c, \omega_c, \ell$.

If we now turn to the graphene QHE system, the same analysis is performed based on Fig.3. The frequency dependence of the transition width is rather similar to that for the 2DEG system, as far as the potential disorder assumed here is concerned. The localization exponent ν and the dynamical critical exponent z for the graphene system are determined as $\nu = 2.1 \pm 0.1$ $z = 1.8 \pm 0.2$, which coincide, within numerical errors, with those for the conventional QHE system. This suggests that the two systems are in the same universality class. As far as the dynamical exponent is concerned, it has been argued by Hikami and Wegner¹⁹ that, when the density of states is an analytic function of energy at a critical point, then $z = d$ (d : spatial dimension, which is 2 in the present case). Thus the fact that we get $z \approx 2$ for the 2DEG QHE is commensurate with this conjecture. On the other hand, the density of states for Dirac fermions ($\rho(E) \sim |E|$ for the clean system) is non-analytic, for which one might expect a different behavior in graphene. The absence of deviation in the value of z in Dirac fermions here should come from the fact that the presence of disorder smears the Dirac cone structure in the density of states to make it smooth (Fig.1(b), inset).

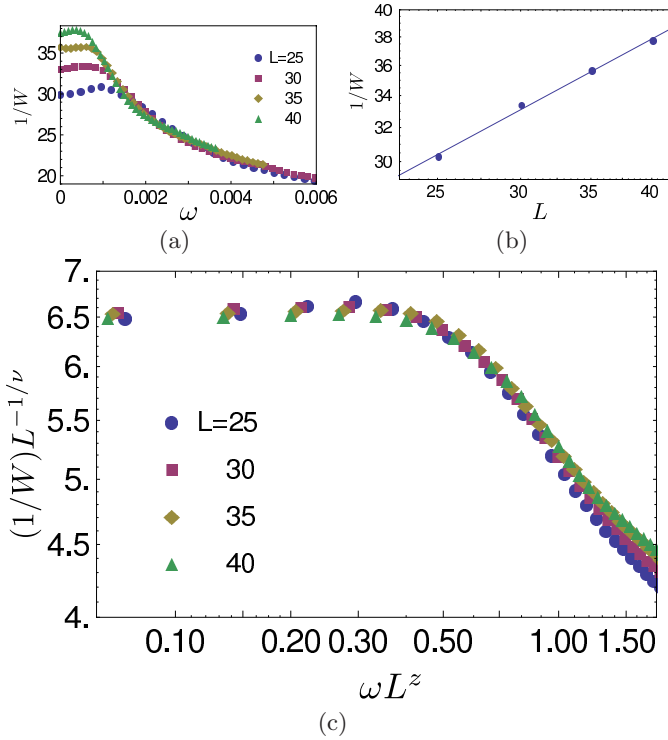


FIG. 3: Dynamical scaling analysis for the graphene QHE system with $\Gamma = 0.4\hbar\omega_c$ and $L = 25 - 40$: (a) The inverse width $1/W$ plotted against the frequency ω , (b) the inverse width $1/W$ plotted against the sample size L , from which the localization exponent $\nu = 2.1 \pm 0.1$ is obtained, and (c) rescaled inverse width $\frac{1}{W}L^{-1/\nu}$ plotted against the rescaled frequency ωL^z with a fitted dynamical critical exponent $z = 1.8 \pm 0.2$.

Having derived the static and dynamic exponents, we can now actually plot the scaling of the rescaled inverse width against rescaled frequency. This is displayed in Fig.2(c) for 2DEG, and Fig.3(c) (for graphene QHE). It can be judged that the scaling fit is quite good, which indicates that the form of the universal function assumed in eqn(7) is adequate. In the scaling plot we can see more clearly the first region with a constant $\frac{1}{W}L^{-1/\nu}$ for small ωL^z , and the second region with a monotonously decreasing $1/W$ for larger ωL^z .

Intuitively, we can elaborate as follows: The dynamical response of the QHE system is governed by the magnitude of the localization length relative to two length scales: the system size L , and the length L_ω which is

the distance over which an electron travels during one cycle, $1/\omega$, of the ac field. Since the localization length diverges as $\xi \sim |\varepsilon - \varepsilon_c|^\nu$ near the center of LL, and the states contributing to $\sigma_{xy}(\omega)$ should be those that simultaneously satisfy $\xi > L$ and $\xi > L_\omega$, the transition width is determined by the smaller length scale L or L_ω . In the static limit $\omega = 0$, with $L_\omega \rightarrow \infty$, the system size L determines the transition width W ¹⁷. When ω is increased, L_ω decreases. In the low enough frequency region, one still has $L_\omega > L$ so that the transition width continues to be determined by the system size. When $L_\omega < L$ for higher frequencies, however, W begins to be governed by L_ω , and the transition width broadens monotonically with frequency. For even higher frequencies, L_ω becomes so small that the system is far from the critical region, and departure from the scaling should occur.

From the functional form of $f(\omega L^z)$ in eqn(7), the frequency for which $\omega L^z \sim 1$, corresponds to the crossover region where the two regions overlap, that is, $L_\omega \sim L$, or $L_\omega \sim 1/\omega^{1/z}$. With the dynamical scaling argument with $z \simeq 2$, we end up with $L_\omega \sim 1/\omega^{1/2} \sim t^{1/2}$ where t is the diffusion time. Since square-root time evolution is a characteristic of diffusion processes, the dynamical response behavior indicates that the present disordered system is diffusive.

The dynamical scaling here enables us to give an estimate of the transition width W in the THz region (with typically $\omega \sim 0.1\omega_c$). In the L_ω -dominated regime, one obtains $W \propto \omega^{1/z\nu}$. The proportionality constant can be read out from the numerical result, Fig. 2(c), so that $W/\hbar\omega_c \sim 0.2\omega^{1/z\nu} \sim 0.1$ at $\omega = 0.1\omega_c$. This implies that the plateau structure remains robust up to the THz region, so that experimental measurements should be feasible.

To summarize, dynamical scaling analysis of the optical Hall conductivity in 2DEG and graphene quantum Hall systems have been carried out, while previous studies have focused mainly on the longitudinal conductivity. The dynamical critical exponent $z \simeq 2$ implies that the system is in the diffusive limit. The dynamical critical exponent z is found to be similar between the 2DEG and the graphene QHE system, but we have to re-emphasize that this is as far as the potential disorder taken here is concerned. It is well-known²⁰ that the preservation or otherwise of the chiral symmetry in disordered graphene has a profound effect on the $n = 0$ graphene Landau level. Thus it is an interesting future problem to look into this effect in terms of the dynamical scaling.

¹ D. J. Thouless, M. Kohmoto, M. P. Nightingale, and M. den Nijs, Phys. Rev. Lett. **49**, 405 (1982).

² Y. Hatsugai, Phys. Rev. Lett. **71**, 3697 (1993).

³ V. Volkov and S. Mikhailov, JETP Letters **41**, 476 (1985).

⁴ T. Morimoto, Y. Hatsugai, and H. Aoki, Phys. Rev. Lett. **103**, 116803 (2009).

⁵ I. V. Fialkovsky and D. V. Vassilevich, J. Phys. A: Math. Theor. **42**, 442001 (2009).

⁶ B. Huckestein, Rev. Mod. Phys. **67**, 357 (1995).

⁷ B. M. Gammel and W. Brenig, Phys. Rev. B **53**, R13279 (1996).

⁸ K. Novoselov, A. Geim, S. Morozov, D. Jiang, M. Katsnel-

- son, I. Grigorieva, S. Dubonos, and A. Firsov, *Nature* **438**, 197 (2005).
- ⁹ S. Koch, R. Haug, K. Klitzing, and K. Ploog, *Phys. Rev. Lett.* **67**, 883 (1991).
- ¹⁰ F. Hohls, U. Zeitler, R. Haug, R. Meisels, K. Dybko, and F. Kuchar, *Phys. Rev. Lett.* **89**, 276801 (2002).
- ¹¹ Y. Ikebe and R. Shimano, *Appl. Phys. Lett.* **92**, 012111 (2008).
- ¹² Y. Ikebe, T. Morimoto, R. Masutomi, T. Okamoto, H. Aoki, and R. Shimano, *arXiv:1004.0308* (2010).
- ¹³ M. L. Sadowski, G. Martinez, M. Potemski, C. Berger, and W. A. de Heer, *Phys. Rev. Lett.* **97**, 266405 (2006).
- ¹⁴ T. Morimoto, Y. Hatsugai, and H. Aoki, *Phys. Rev. B* **78**, 073406 (2008).
- ¹⁵ T. Ando, *J. Phys. Soc. Jpn.* **38**, 989 (1975).
- ¹⁶ K. Nomura, S. Ryu, M. Koshino, C. Mudry, and A. Furusaki, *Phys. Rev. Lett.* **100**, 246806 (2008).
- ¹⁷ H. Aoki and T. Ando, *Phys. Rev. Lett.* **54**, 831 (1985).
- ¹⁸ Y. Avishai and J. Luck, *arXiv:cond-mat/9609265* (1996).
- ¹⁹ F. Wegner in Y. Nagaoka and H. Fukuyama, eds., *Anderson Localization* (Springer, 1982), p.8; S. Hikami, *ibid*, p.15.
- ²⁰ T. Kawarabayashi, Y. Hatsugai, and H. Aoki, *Phys. Rev. Lett.* **103**, 156804 (2009).
- ²¹ To be precise, we have included a slight shift of the center of the tanh function to have a better fit, but the shift is tiny $\sim 0.001\hbar\omega_c$.